Article

Immunity

Macrophage Akt1 Kinase-Mediated Mitophagy Modulates Apoptosis Resistance and Pulmonary Fibrosis

Graphical Abstract

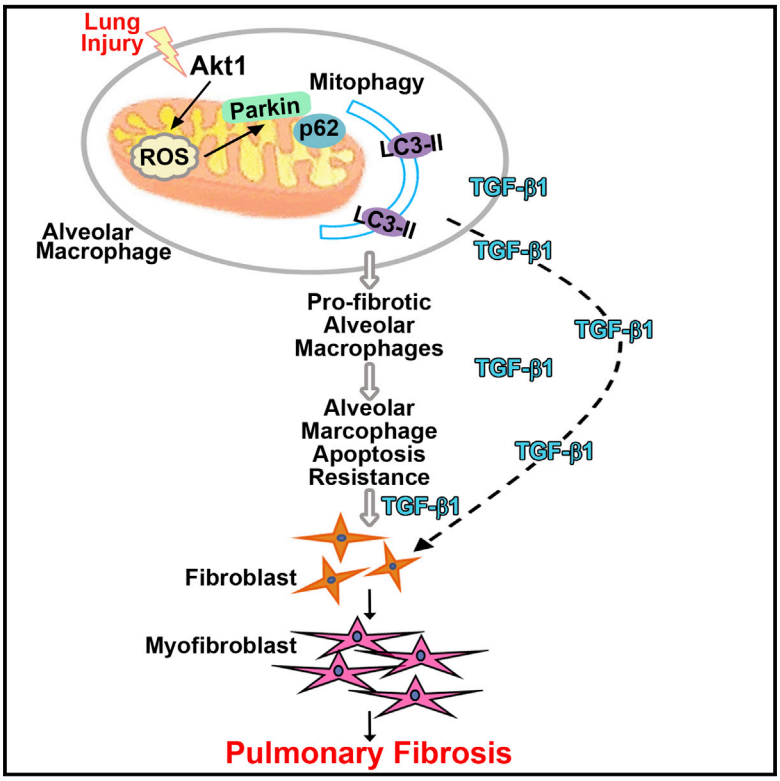

Highlights

- IPF alveolar macrophages undergo mitophagy and display apoptosis resistance
- Akt1-mediated mitochondrial ROS induce mitophagy and apoptosis resistance
- Mitophagy is required for apoptosis resistance and TGF-β1 expression in macrophages
- Macrophage-derived TGF-β1 is required for pulmonary fibrosis

Authors

Jennifer L. Larson-Casey, Jessy S. Deshane, Alan J. Ryan, Victor J. Thannickal, A. Brent Carter

Correspondence

bcarter1@uab.edu

In Brief

Alveolar macrophage Akt1 is required in the pathogenesis of pulmonary fibrosis. Carter and colleagues demonstrate that dysfunctional mitochondria are removed in alveolar macrophages expressing Akt1 and promote apoptosis resistance during the fibrotic process. Furthermore, Akt1-mediated mitophagy modulates the effector cells, myofibroblasts, via TGF-β1 production by alveolar macrophages.

Larson-Casey et al., 2016, Immunity *44*, 582–596
March 15, 2016
http://dx.doi.org/10.1016/j.immuni.2016.01.001

CellPress

CellPress

Immunity
Article

Macrophage Akt1 Kinase-Mediated Mitophagy Modulates Apoptosis Resistance and Pulmonary Fibrosis

Jennifer L. Larson-Casey,[1] Jessy S. Deshane,[1] Alan J. Ryan,[2] Victor J. Thannickal,[1,3] and A. Brent Carter[1,3,4,*]
[1]Department of Medicine, Division of Pulmonary, Allergy, and Critical Care Medicine, University of Alabama at Birmingham, Birmingham, AL 35294, USA
[2]Department of Internal Medicine, University of Iowa, Iowa City, IA 52242, USA
[3]Birmingham Veterans Administration Medical Center, Birmingham, AL 35294, USA
[4]Present address: 1918 University Blvd, 404 MCLM, Department of Medicine, University of Alabama at Birmingham, Birmingham, AL 35294, USA
*Correspondence: bcarter1@uab.edu
http://dx.doi.org/10.1016/j.immuni.2016.01.001

SUMMARY

Idiopathic pulmonary fibrosis (IPF) is a devastating lung disorder with increasing incidence. Mitochondrial oxidative stress in alveolar macrophages is directly linked to pulmonary fibrosis. Mitophagy, the selective engulfment of dysfunctional mitochondria by autophagasomes, is important for cellular homeostasis and can be induced by mitochondrial oxidative stress. Here, we show Akt1 induced macrophage mitochondrial reactive oxygen species (ROS) and mitophagy. Mice harboring a conditional deletion of Akt1 in macrophages (*Akt1*$^{-/-}$*Lyz2-cre*) and *Park2*$^{-/-}$ mice had impaired mitophagy and reduced active transforming growth factor-β1 (TGF-β1). Although Akt1 increased TGF-β1 expression, mitophagy inhibition in Akt1-overexpressing macrophages abrogated TGF-β1 expression and fibroblast differentiation. Importantly, conditional *Akt1*$^{-/-}$*Lyz2-cre* mice and *Park2*$^{-/-}$ mice had increased macrophage apoptosis and were protected from pulmonary fibrosis. Moreover, IPF alveolar macrophages had evidence of increased mitophagy and displayed apoptosis resistance. These observations suggest that Akt1-mediated mitophagy contributes to alveolar macrophage apoptosis resistance and is required for pulmonary fibrosis development.

INTRODUCTION

Pulmonary fibrosis is a devastating disorder that has an increasing prevalence of over 60 per 100,000 persons, and the cost of care has had a dramatic upward trend in recent years (Collard et al., 2015; Collard et al., 2012). This devastating disease has a median life expectancy of 3-5 years after diagnosis for certain forms of pulmonary fibrosis, such as idiopathic pulmonary fibrosis (IPF) (Collard et al., 2012; Raghu et al., 2004; Schwartz et al., 1994). Unfortunately, there are no current therapies to halt the development and/or progression of pulmonary fibrosis; thus, understanding the basic molecular mechanisms might uncover additional therapeutic modalities.

Alveolar macrophages play an integral role in the pathogenesis of pulmonary fibrosis by initiating an immune response and generating reactive oxygen species (ROS). Lung remodeling during pulmonary fibrosis is poorly understood, but the generation of ROS, particularly mitochondrial H_2O_2, from alveolar macrophages plays an integral role in fibrosis development by increasing the expression of transforming growth factor-β (TGF-β1) (He et al., 2011; Jain et al., 2013). The abrogation of mitochondrial oxidative stress reduces *Tgfb1* and attenuates the development of pulmonary fibrosis in mice (He et al., 2011; Osborn-Heaford et al., 2012).

Protein kinase B, or Akt1, a pro-survival kinase, is known to mediate mitochondrial H_2O_2 generation (Larson-Casey et al., 2014), and mitochondrial ROS plays an important role in macrophage innate immunity (West et al., 2011). Although mitochondrial ROS is usually considered toxic, it also has beneficial effects, such as modulating mitochondrial dynamics. For example, mitophagy, a form of macroautophagy, is the selective engulfment of dysfunctional mitochondria by autophagosomes and can be induced by mitochondrial ROS (Chen et al., 2009; Lee et al., 2011; Patel et al., 2015; Wang et al., 2012). Mitochondrial dysfunction results in PTEN-induced putative kinase 1 (PINK1) binding to the outer mitochondrial membrane where it recruits the E3 ubiquitin ligase Parkin (Narendra et al., 2008). These mitochondria are targeted for mitophagy that is dependent on Parkin-mediated ubiquitination of mitochondrial proteins. Thus, mitophagy is important for the quality control of the mitochondrial population and cell homeostasis.

Mitophagy is present in several lung diseases, such as lung cancer, sepsis-induced acute lung injury, and chronic obstructive pulmonary disease (Chang et al., 2015; Chen et al., 2014; Mizumura et al., 2014). In type II alveolar epithelial cells from the IPF lung, PINK1 expression is decreased, while no difference is seen in IPF lung fibroblasts compared to normal subjects (Bueno et al., 2015). However, PINK1 protein is increased in IPF whole lung homogenates (Patel et al., 2015). The role mitophagy plays in alveolar macrophages in pulmonary fibrosis has not been determined. Our data show that mitophagy contributes to

alveolar macrophage apoptosis resistance and is required for macrophage-derived *Tgfb1* expression and is modulated, in part, by Akt1 activation.

RESULTS

Alveolar Macrophage Akt1 Is Required for the Development of Pulmonary Fibrosis

Because Akt is often altered in human disease and can be activated by many cellular stimuli or toxic insults (Govindarajan et al., 2007; Larson-Casey et al., 2014), we measured the expression of Akt1 in alveolar macrophages from normal subjects and IPF patients. Alveolar macrophages showed a 3-fold increase of p-Akt1 in IPF patients compared to normal subjects (Figures 1A and 1B).

To investigate the relationship of macrophage Akt1 activation to pulmonary fibrosis in vivo, we subjected WT and $Akt1^{+/-}$ mice to bleomycin-induced lung injury. Alveolar macrophages from $Akt1^{+/-}$ mice had a decrease in p-Akt1 expression compared to WT mice (Figure 1C). Lungs from WT mice showed widespread destruction of lung architecture and aberrant collagen deposition (Figure 1D), whereas $Akt1^{+/-}$ mice had a marked reduction in collagen accumulation and preserved lung architecture (Figure 1E). The histological findings were verified biochemically by hydroxyproline assay (Figure 1F).

We assessed whether Akt1 was activated in alveolar macrophages from fibrotic mice. Macrophages isolated from the lungs of bleomycin-injured mice had increased p-Akt1 expression (Figure 1G), which was 5-fold greater compared to control mice (Figure 1H). The PI3K inhibitor, LY294002, inhibited phosphorylation of Akt1 and the PI3K regulatory subunit (p85) at Tyr^{458}, which is necessary for Akt1 activation (Figure S1A). Alveolar macrophages from bleomycin-injured WT mice had increased phosphorylation of p85 (Figure S1B).

To investigate the pathological significance of macrophage Akt1 in fibrosis, we generated mice harboring a conditional deletion of Akt1 in macrophages ($Akt1^{-/-}$*Lyz2-cre*). Alveolar macrophages isolated from $Akt1^{-/-}$*Lyz2-cre* mice had a complete absence of p-Akt1 and Akt1 expression, whereas bleomycin-injured WT mice showed an increase in p-Akt1 expression (Figure 1I). Type II alveolar epithelial cells isolated from WT and $Akt1^{-/-}$*Lyz2-cre* mice had similar expression of p-Akt1 and Akt1, suggesting efficient recombination only in macrophages (Figure S1C). WT and $Akt1^{-/-}$*Lyz2-cre* mice had similar numbers of BAL cells after bleomycin (Figure S1D); however, WT mice had greater loss of barrier function, indicating more lung injury (Figure S1E).

The conditional deletion of Akt1 from alveolar macrophages had no effect on the lung parenchyma in saline-exposed mice (Figures 1J and 1K). There was dense collagen deposition in bleomycin-injured WT mice (Figure 1L), whereas the $Akt1^{-/-}$*Lyz2-cre* mice had essentially normal lungs (Figure 1M). The histological findings were confirmed biochemically (Figure 1N). These data suggest that Akt1 activation in alveolar macrophages is required in the pathogenesis of bleomycin-induced pulmonary fibrosis.

IPF Patients Have Increased Pro-Fibrotic Alveolar Macrophages

Pro-fibrotic macrophages are responsible for the generation of anti-inflammatory cytokines and are often associated with fibrotic conditions, including pulmonary fibrosis (He et al., 2013; Redente et al., 2014). We questioned whether alveolar macrophages from IPF patients have a predominant pro-fibrotic phenotype. Mannose receptor (Figure 2A) and interleukin-10 (IL-10) (Figure 2B) mRNA expression were more than 6-fold and 300-fold greater in IPF alveolar macrophages. Moreover, TGF-β1 mRNA expression in alveolar macrophages was greater than 7-fold more in IPF patients compared to normal volunteers (Figure 2C).

Because the deletion of Akt1 in macrophages in vivo is protective, we hypothesized that Akt1 expression led to the polarization of macrophages to a pro-fibrotic phenotype. The pro-fibrotic marker, Ym1, was significantly increased in the BAL fluid from bleomycin-injured WT mice (Figure 2D). In contrast, $Akt1^{-/-}$*Lyz2-cre* mice had Ym1 concentrations below controls. Furthermore, active TGF-β1 in the BAL fluid from $Akt1^{-/-}$*Lyz2-cre* mice was similar to saline controls from WT mice (Figure 2E). The anti-fibrotic markers (tumor necrosis factor alpha [TNF-α], IL-1β, and IL-6) had an opposite expression trend in BAL fluid (Figures S2A–S2C).

Because TGF-β1 is known to induce differentiation of fibroblasts to myofibroblasts, we determined whether BAL fluid from mice promoted IPF fibroblast differentiation. IPF fibroblasts incubated with BAL fluid from WT mice induced an increase in α-smooth muscle actin (α-SMA) (Figures 2F and 2G). The α-SMA expression was less in fibroblasts incubated with BAL fluid from $Akt1^{-/-}$*Lyz2-cre* mice than WT controls suggesting that macrophage-derived TGF-β1 production is critical for fibroblast differentiation.

The difference in fibroblast differentiation correlated with altered myofibroblast function. IPF fibroblasts incubated in BAL fluid from bleomycin-injured WT mice showed a 29,000-fold increase in fibronectin (Figure 2H) and 400-fold increase in collagen 1α mRNA compared to IPF fibroblasts incubated in BAL fluid from $Akt1^{-/-}$*Lyz2-cre* mice (Figure 2I). Normal human lung fibroblasts showed a similar trend (Figures S2D and S2E). Taken together, these data suggest that alveolar macrophages from $Akt1^{-/-}$*Lyz2-cre* mice are anti-fibrotic and have reduced production of the pro-fibrotic factor(s) required for myofibroblast function.

Macrophage-Derived TGF-β1 Is Required for Pulmonary Fibrosis

On the basis of these observations in fibroblast differentiation and function, we hypothesized that these findings were due to decreased macrophage-derived TGF-β1 in $Akt1^{-/-}$*Lyz2-cre* mice. To determine whether macrophage TGF-β1 mediated these changes, we generated mice harboring a conditional deletion of *Tgfb1* in macrophages ($Tgfb1^{-/-}$ *Lyz2-cre*). Bleomycin-injured WT mice had a 4-fold increase in TGF-β1 mRNA expression compared to saline controls, while TGF-β1 mRNA expression in $Tgfb1^{-/-}$*Lyz2-cre* mice was at the limit of detection (Figure 3A). Confirming these results, active TGF-β1 measured in BAL fluid in $Tgfb1^{-/-}$*Lyz2-cre* mice was below WT saline controls (Figure 3B). The total number of BAL cells was increased with bleomycin exposure (Figure 3C), and alveolar macrophages were the predominant (> 90%) cell type (Figure 3D).

Trichrome staining revealed deletion of TGF-β1 from alveolar macrophages had no effect on lung parenchyma,

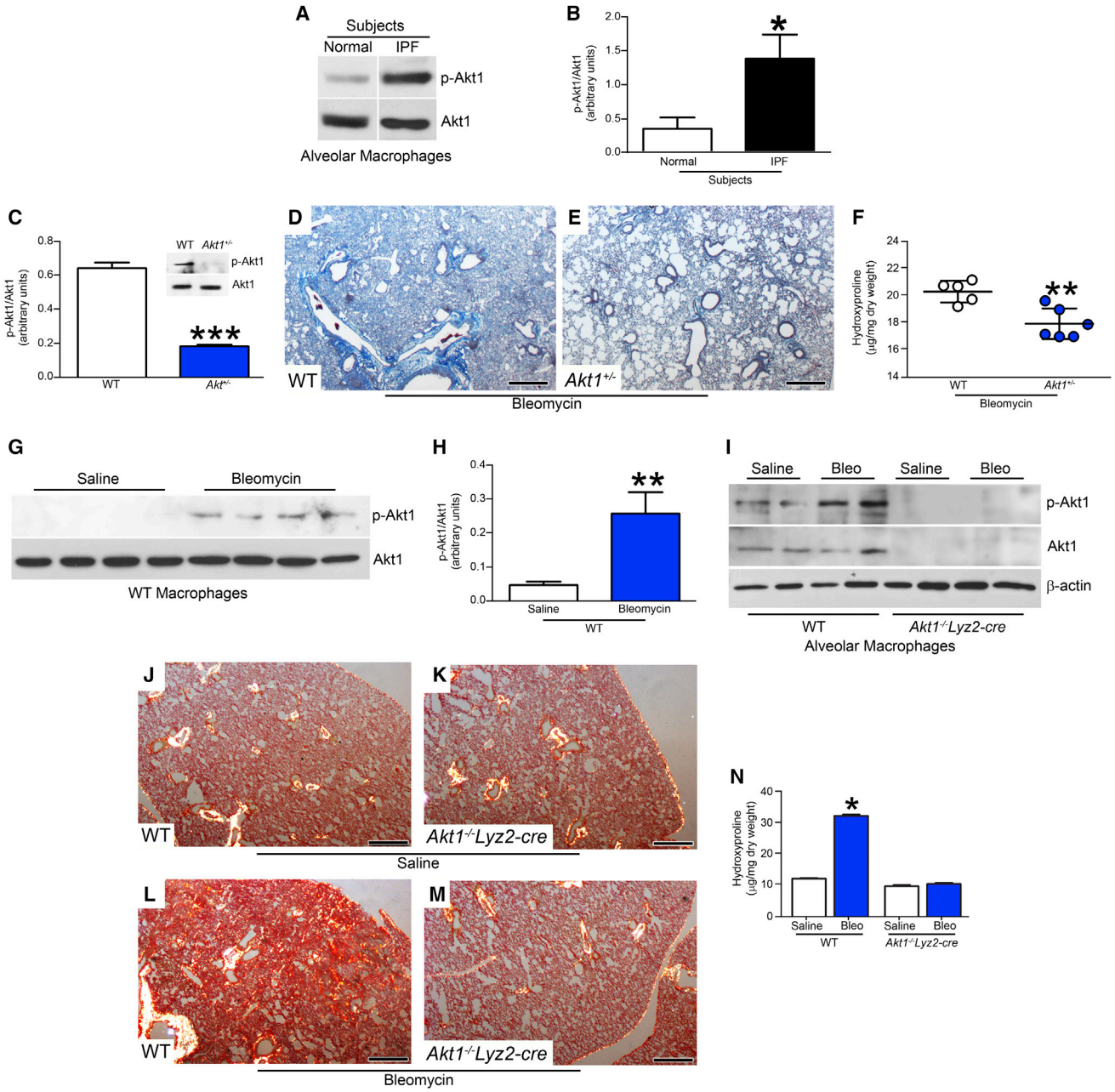

Figure 1. Akt1 Activation in Alveolar Macrophages Is Associated with Pulmonary Fibrosis

(A) Immunoblot and (B) densitometric analysis of alveolar macrophages isolated by BAL from normal subjects (n = 4) and IPF patients (n = 5), Student's t test.

(C) Quantitative analysis and representative immunoblot (Inset) of alveolar macrophages isolated by BAL from WT (n = 5) and *Akt1*$^{+/-}$ mice (n = 5) exposed to bleomycin (2 U/kg) intratracheally, Student's t test.

(D and E) After bleomycin exposure, mice were euthanized 21 days later and lungs from (D) WT and (E) *Akt1*$^{+/-}$ mice were removed and processed for Masson's trichrome staining. Representative micrographs from 1 of 6 mice are shown. Scale bar represents 600 μm.

(F) Hydroxyproline assay of lungs removed from WT (n = 5) and *Akt1*$^{+/-}$ mice (n = 6) after bleomycin exposure, Student's t test. WT mice were exposed to saline (n = 4) or bleomycin (n = 5) intratracheally, BAL was performed 21 days later.

(G) Immunoblot and (H) densitometry analysis. Student's t test.

(I) Immunoblot analysis of macrophages isolated by BAL from WT (n = 4 saline; n = 5 bleo) and *Akt1*$^{-/-}$*Lyz2-cre* mice (n = 4 saline; n = 6 bleo).

(J–M) Excised lungs from WT and *Akt1*$^{-/-}$*Lyz2-cre* mice exposed to (J) and (K) saline or (L) and (M) bleomycin were stained with Sirius red. Representative micrographs from WT (n = 4 saline; n = 5 bleo) and *Akt1*$^{-/-}$*Lyz2-cre* mice (n = 4 saline; n = 7 bleo) are shown. Scale bar represents 500 μm.

(**N**) Hydroxyproline of lungs from WT (n = 4 saline; n = 5 bleo) and *Akt1*$^{-/-}$*Lyz2-cre* mice (n = 4 saline; n = 6 bleo). One-way ANOVA with Tukey's comparison. *p < 0.05; **p < 0.002; ***p < 0.0001. Values are mean ± SD of a minimum of three independent experiments performed in triplicate. Please see Figure S1.

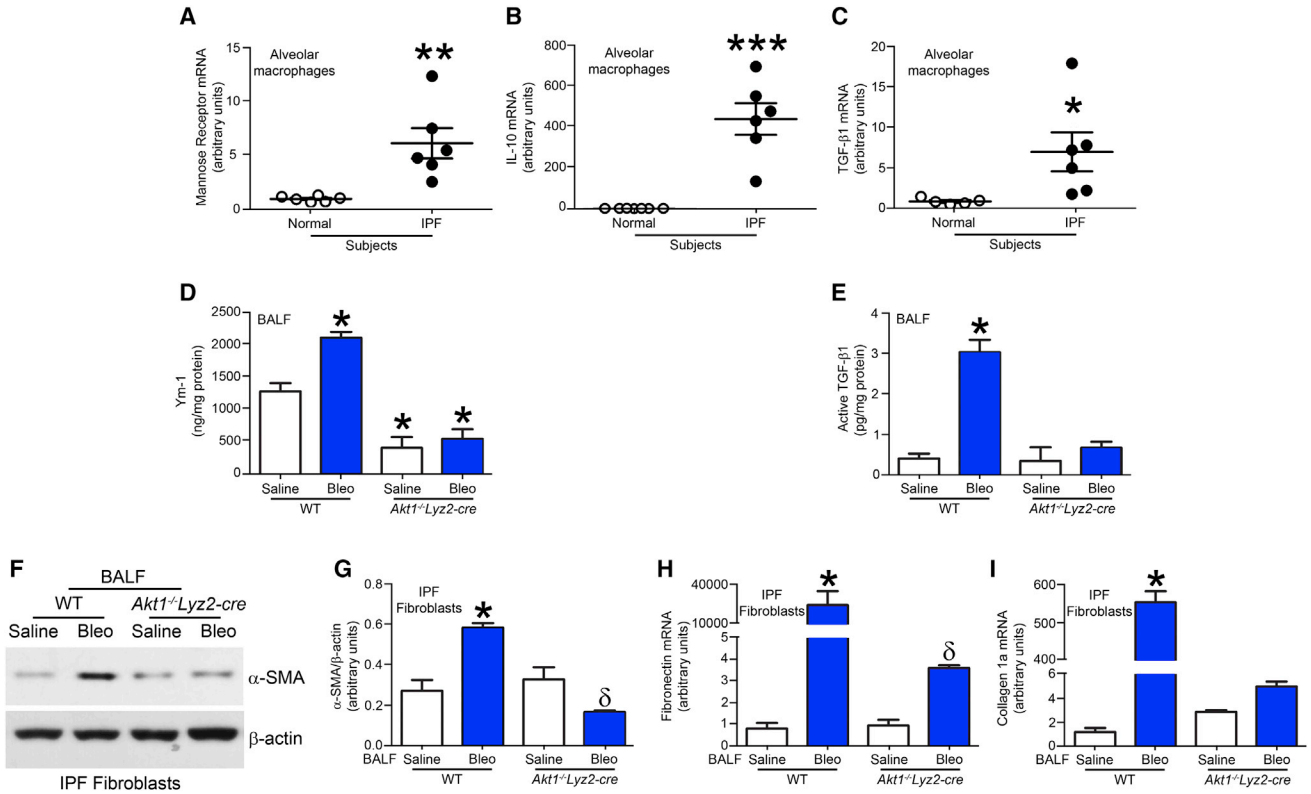

Figure 2. Alveolar Macrophages from IPF Patients Have a Pro-Fibrotic Phenotype

Total RNA was isolated from alveolar macrophages obtained from normal subjects and IPF patients by BAL.

(A) Mannose receptor (n = 6), (B) IL-10 (n = 7 normal; n = 6 IPF), and (C) TGF-β1 mRNA (n = 5 normal; n = 6 IPF) were measured by quantitative PCR, Student's t test. WT and *Akt1*$^{-/-}$*Lyz2-cre* mice were exposed to saline or bleomycin (bleo) intratracheally and BAL was performed 21 days later.

(D) Ym-1 and (E) Active TGF-β1 were measured in BAL fluid by ELISA. n = 4 saline; n = 5 bleo.

(F) Immunoblot and (G) densitometry analysis of IPF fibroblasts cultured in BAL fluid from exposed WT and *Akt1*$^{-/-}$*Lyz2-cre* mice. n = 3 saline; n = 4 bleo. Total RNA was isolated from IPF fibroblasts conditioned with BAL fluid from WT and *Akt1*$^{-/-}$*Lyz2-cre* mice.

(H) Fibronectin and (I) collagen *1A* mRNA were measured. n = 4 saline; n = 5 bleo. *p < 0.05 versus WT+saline; **p < 0.001; ***p < 0.0001; δ, p < 0.05 versus *Akt1*$^{-/-}$*Lyz2-cre* +saline. One-way ANOVA with Tukey's comparison. Values are mean ± SD of a minimum of three independent experiments performed in triplicate. Please see Figure S2.

verifying that macrophage-derived TGF-β1 mediates lung fibrosis (Figures 3E and 3F). Bleomycin-injured WT mice had widespread accumulation of collagen in lungs (Figure 3G), whereas *Tgfb1*$^{-/-}$*Lyz2-cre* mice had normal lung architecture similar to saline controls (Figure 3H). These results were confirmed by hydroxyproline assay (Figure 3I). Bleomycin increased p-Akt1 in alveolar macrophages from WT and *Tgfb1*$^{-/-}$*Lyz2-cre* mice, although the conditional deletion of *Tgfb1* resulted in greater expression of p-Akt1 (Figure S3A). Moreover, alveolar macrophages isolated from *Tgfb1*$^{-/-}$*Lyz2-cre* mice polarize to an anti-fibrotic phenotype, with increased IL-1β, IL-6, and TNF-α and decreased Ym-1 mRNA expression compared to WT mice (Figures S3B–S3E).

Further evidence to support the role of macrophage-derived TGF-β1 in development of a fibrotic phenotype is that α-SMA was attenuated in IPF fibroblasts incubated in *Tgfb1*$^{-/-}$*Lyz2-cre* BAL fluid compared to WT saline controls (Figures 3J and 3K). These observations support the notion that macrophage-derived active TGF-β1 expression mediates development of a fibrotic phenotype in vivo.

Mitophagy Is Increased in IPF Alveolar Macrophages

Studies have conflicting data on the role of mitophagy in type II alveolar epithelial cells and fibroblasts from IPF patients (Araya et al., 2013; Bueno et al., 2015; Kim et al., 2012; Patel et al., 2015; Ricci et al., 2013); however, the contribution of mitophagy in alveolar macrophages to fibrosis development is not known. We found that mitochondria isolated from IPF alveolar macrophages had greater immunoreactive PINK1 (Figures 4A and 4B) and Parkin expression (Figures 4A and 4C) compared to normal subjects. The increase corresponded to an increase of LC3-II expression in alveolar macrophages (Figures 4D and 4E), suggesting mitophagy is occurring as indicated by autophagosome formation.

We investigated whether macrophage mitophagy was recapitulated in vivo. WT mice with bleomycin-induced injury had increased PINK1 and Parkin expression in isolated mitochondria from alveolar macrophages (Figures 4F–4H), and LC3-II expression was also increased (Figures 4I and 4J). In contrast, *Akt1*$^{-/-}$*Lyz2-cre* mice showed no evidence of PINK1, Parkin, or LC3-II expression.

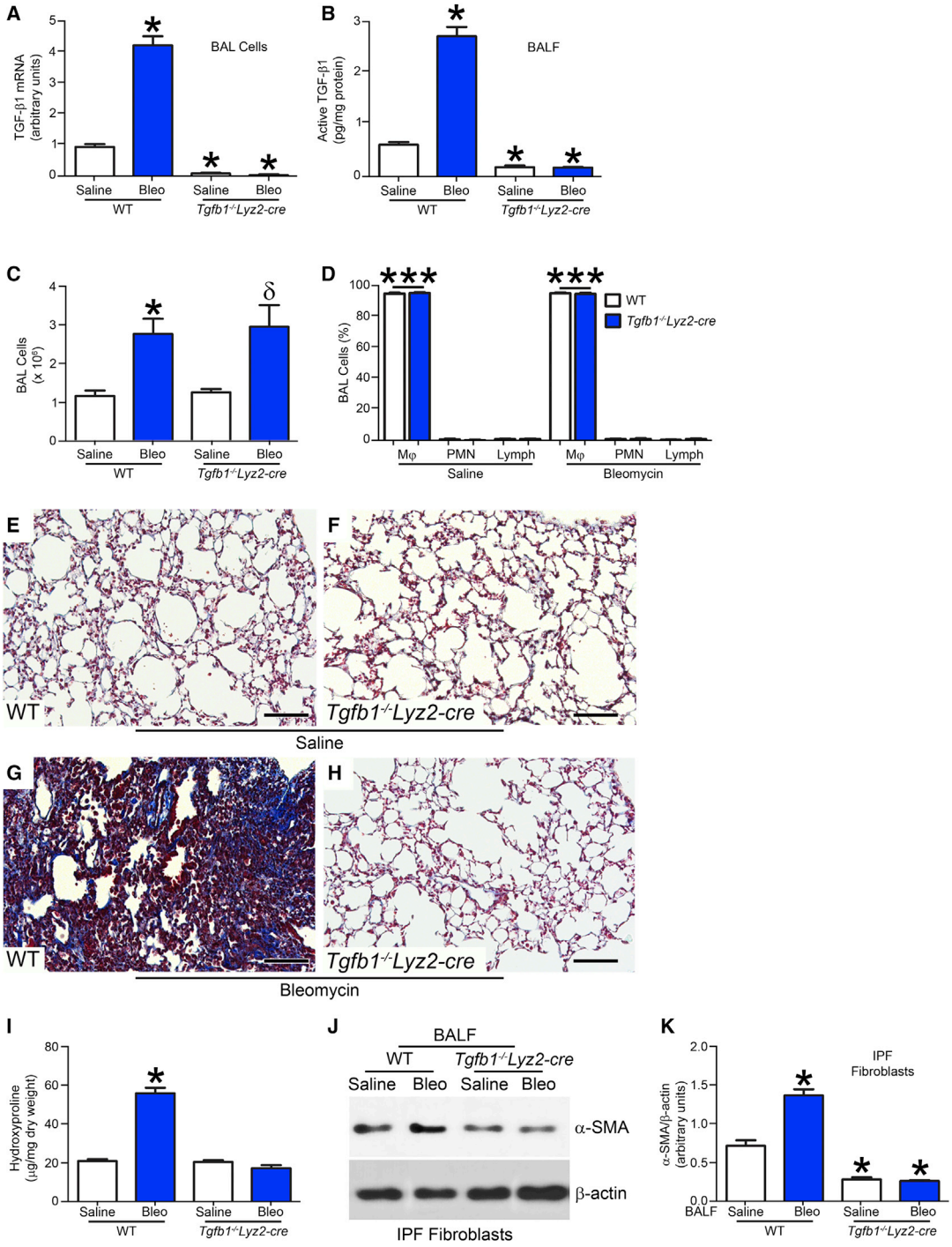

Figure 3. Macrophage-Derived TGF-β1 Is Required for Pulmonary Fibrosis

WT and *Tgfb1*$^{-/-}$ *Lyz2-cre* mice were exposed to saline or bleomycin intratracheally and BAL was performed 21 days later.

(A) Total RNA was isolated from alveolar macrophages obtained by BAL. TGF-β1 mRNA was measured.

(B) Active TGF-β1 was measured in BAL fluid by ELISA from WT and *Tgfb1*$^{-/-}$ *Lyz2-cre* mice; n = 6.

(C) Total number of BAL cells and (D) cell differential determined using Wright-Giemsa stain from BAL; n = 6. Lungs were excised from WT and *Tgfb1*$^{-/-}$ *Lyz2-cre* mice exposed to (E) and (F) saline or (G) and (H) bleomycin and stained using Masson's trichrome. Representative micrographs from WT and *Tgfb1*$^{-/-}$ *Lyz2-cre* mice; n = 6. Scale bar represents 200 μm.

(I) Hydroxyproline of lungs removed from WT and *Tgfb1*$^{-/-}$ *Lyz2-cre* mice; n = 6.

(J) Immunoblot and (K) densitometry analysis of IPF fibroblasts cultured in BAL fluid from exposed WT and *Tgfb1*$^{-/-}$ *Lyz2-cre* mice; n = 6. *$p < 0.05$ versus WT+saline; ***$p < 0.0001$ versus PMN and Lymph. One-way ANOVA with Tukey's comparison. Values are mean ± SD of a minimum of three independent experiments performed in triplicate. Please see Figure S3.

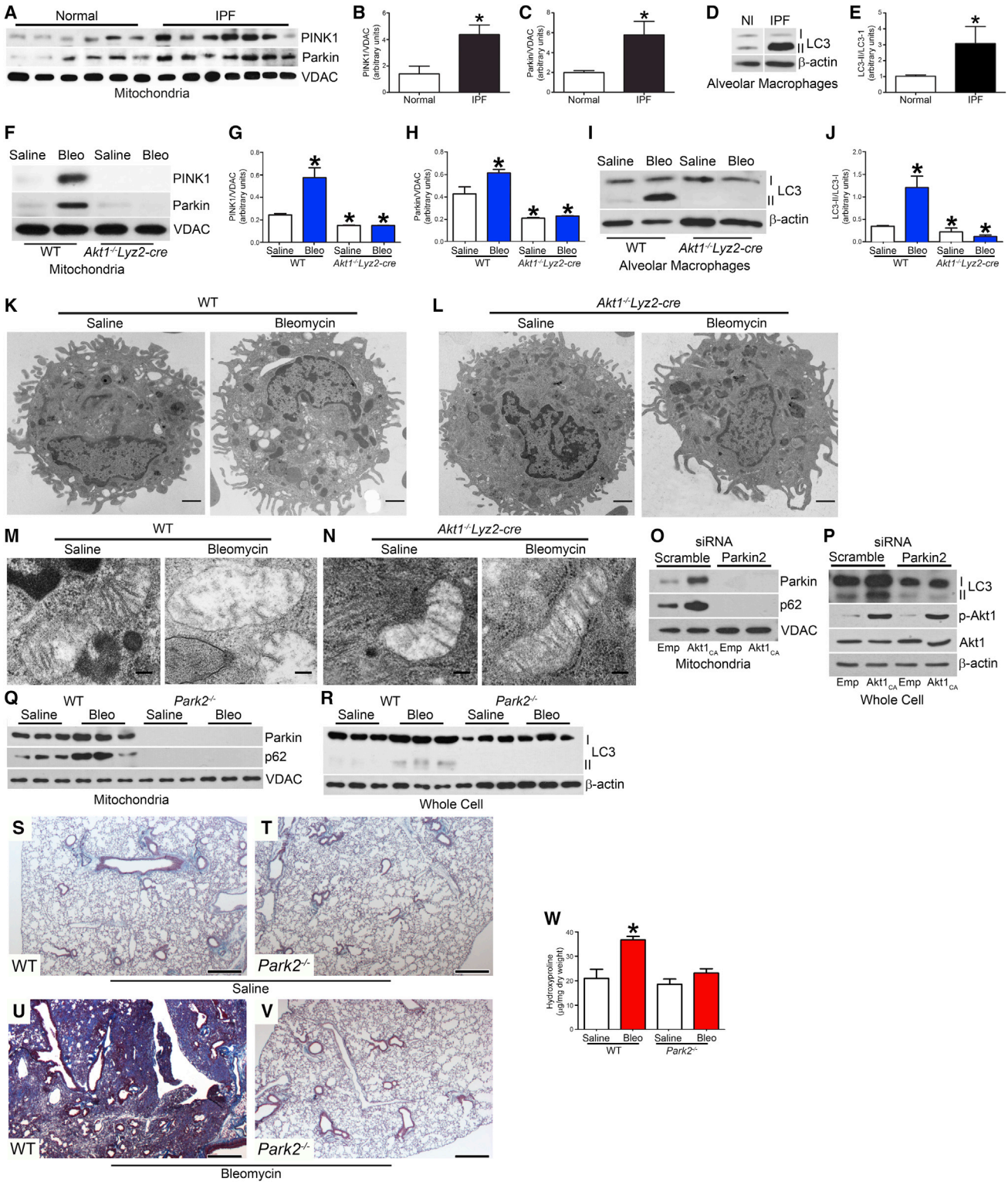

Figure 4. Mitophagy Is Enhanced in Pro-Fibrotic Alveolar Macrophages

(A) Mitochondria isolated from alveolar macrophages from normal subjects (n = 6) and IPF patients (n = 7) were subjected to immunoblot analysis.

(B and C) Densitometry analysis of (B) PINK1 and (C) Parkin immunoblots normalized to VDAC, Student's t test. Alveolar macrophages from normal subjects (n = 7) and IPF patients (n = 6) were subjected to (D) immunoblot and (E) densitometry analysis, Student's t test.

(legend continued on next page)

To determine the effect of Akt1 expression in alveolar macrophages visually, we used transmission electron microscopy to examine alveolar macrophage mitophagy. Bleomycin increased the presence of vacuoles in alveolar macrophages isolated from bleomycin-injured WT mice compared to macrophages isolated from saline controls (Figure 4K). Conversely, alveolar macrophages isolated from *Akt1*$^{-/-}$*Lyz2-cre* mice had no visualized vacuoles (Figure 4L). Bleomycin-injured WT alveolar macrophages had mitochondria with an irregular shape and disorganized cristae (Figure 4M), whereas alveolar macrophages isolated from *Akt1*$^{-/-}$*Lyz2-cre* mice had normal mitochondria (Figure 4N). Overexpression of constitutive active Akt1 (Akt1$_{CA}$) in macrophages in vitro increased the number of vacuoles compared to the saline controls, confirming this difference was Akt1-mediated (Figures S4A and S4B). Vacuole number increased dramatically in cells expressing Akt1$_{CA}$ after bleomycin treatment. These findings provide direct evidence that Akt1 activation in alveolar macrophages induces mitophagy.

Although increased LC3-II expression suggests induction of autophagy, we analyzed flux through the autophagy–lysosome pathway in macrophages by several methods. Macrophages treated with bafilomycin A (Baf A), an inhibitor of autophagosome fusion with lysosomes, had increased mitochondrial accumulation of PINK1 and Parkin (Figures S4C). The autophagy adaptor protein, p62, and LC3-II expression were increased as well. Overexpression of Akt1$_{CA}$ with Baf A treatment showed a further induction (Figures S4C and S4D). The autophagy inhibitor, 3-methyladenine (3-MA), inhibited autophagy flux in macrophages even in the presence of Akt1$_{CA}$ (Figures S4E and S4F).

Because mitophagy results in degradation of several mitochondrial proteins, including TOM20 (Wauer et al., 2015), cells expressing Akt1$_{CA}$ treated with vehicle had a decrease in TOM20, whereas Baf A treatment increased TOM20 expression in the presence or absence of Akt1$_{CA}$ (Figure S4G). Similar results were obtained with leupeptin, a lysosomal enzyme inhibitor (Figure S4H), providing further evidence that Akt1 regulates macrophage mitophagy.

We evaluated the role of Akt1 using a genetic approach. Mitochondria isolated from Parkin2-deficient macrophages showed an absence of mitophagy with Akt1$_{CA}$ overexpression (Figure 4O). LC3-II expression was also absent with Parkin2 silencing (Figure 4P). We determined the biological relevance of mitophagy inhibition. Alveolar macrophages isolated from bleomycin-treated *Park2*$^{-/-}$ mice showed no Parkin or p62 in isolated mitochondria and no corresponding LC3-II expression (Figures 4Q and 4R).

The deletion of Parkin in vivo did not alter lung architecture (Figures 4S and 4T). Bleomycin-injured WT mice had widespread collagen deposition with destruction of lung architecture (Figure 4U), whereas the bleomycin-treated *Park2*$^{-/-}$ mice had essentially normal lungs (Figure 4V). These results were confirmed by hydroxyproline analysis (Figure 4W). These data suggest that macrophage mitophagy is critical for the pathogenesis of fibrosis.

We determined whether inducing mitophagy had the opposite effect. Alveolar macrophages isolated from rapamycin-treated mice had increased expression of PINK1, Parkin, and p62, as well as LC3-II (Figures S4I and S4J). Moreover, fibrosis development was augmented by rapamycin (Figure S4K).

Akt1-Mediated Mitochondrial ROS in Alveolar Macrophages Induces Mitophagy

One measure of mitochondrial dysfunction and an indicator of mitophagy is the loss of mitochondrial membrane potential ($\Delta\psi_m$) (Narendra et al., 2008; Vives-Bauza et al., 2010). Macrophages exposed to bleomycin showed a loss in $\Delta\psi_m$ (Figure S5A), and increasing concentrations of bleomycin induced a dose-dependent decrease in $\Delta\psi_m$ (data not shown). Overexpression of Akt1$_{CA}$ did not reverse or lead to the loss of $\Delta\psi_m$.

Because mitophagy is induced by ROS and Akt1 increases mitochondrial ROS (Chen et al., 2009; Larson-Casey et al., 2014; Lee et al., 2011; Patel et al., 2015; Wang et al., 2012), we determined that IPF alveolar macrophages had significantly greater mitochondrial H_2O_2 produced while normal subjects showed no difference in H_2O_2 produced in membrane or mitochondrial fractions (Figure 5A). This was also seen in vivo. Mitochondria isolated from bleomycin-injured WT mice produced significantly more H_2O_2 than saline controls (Figure 5B). In contrast, mitochondria isolated from *Akt1*$^{-/-}$*Lyz2-cre* mice had decreased H_2O_2 production compared to WT mice, and there was no increase in H_2O_2 generation with bleomycin. Similar observations were seen in the lungs of mice; bleomycin-injured WT mice had significantly greater percentage of glutathione in its oxidized form, GSSG, than *Akt1*$^{-/-}$*Lyz2-cre* mice (Figure S5B).

To confirm Akt1 mediates mitochondrial ROS, we co-stained macrophages with MitoSOX red and MitoTracker green to quantitate mitochondrial ROS by flow cytometry. Bleomycin increased fluorescence in cells expressing an empty vector (Figure 5C). Overexpression of Akt1$_{CA}$ increased MitoSOX fluorescence to a greater extent than bleomycin alone, and bleomycin

(F) Macrophages isolated from exposed WT and *Akt1*$^{-/-}$*Lyz2-cre* mice were subjected to immunoblot analysis. Quantitative analysis of (G) PINK1 and (H) Parkin immunoblots normalized to VDAC.

(I) Immunoblot and (J) densitometry analysis in alveolar macrophages from exposed WT and *Akt1*$^{-/-}$*Lyz2-cre* mice. WT (n = 4 saline; n = 5 bleo) and *Akt1*$^{-/-}$*Lyz2-cre* mice (n = 4 saline; n = 6 bleo). Macrophages isolated from exposed WT and *Akt1*$^{-/-}$*Lyz2-cre* mice were analyzed by transmission electron microscopy. Images representative of n = 5.

(K and L) Scale bar represents 1 μm.

(M and N) Scale bar represents 100 nm.

(O) Mitochondrial Parkin and p62, and (P) p-Akt1, Akt1, LC3-I and -II expression were measured in THP-1 cells transfected with scrambled or Parkin2 siRNA in combination with empty or Akt1$_{CA}$ vectors. Exposed WT and *Park2*$^{-/-}$ mice were subjected to BAL at day 21. Immunoblot analysis of (Q) mitochondrial Parkin and p62, (R) LC3-I and -II expression were measured. Lungs were excised from WT and *Park2*$^{-/-}$ mice exposed to (S) and (T) saline or (U) and (V) bleomycin and stained with Masson's trichrome. Representative micrographs of 1 of 5 mice are shown. Scale bar represents 500 μm.

(W) Hydroxyproline assay; n = 5. *p < 0.05 versus WT+saline. One-way ANOVA with Tukey's comparison. Values are mean ± SD of a minimum of three independent experiments performed in triplicate. Please see Figure S4.

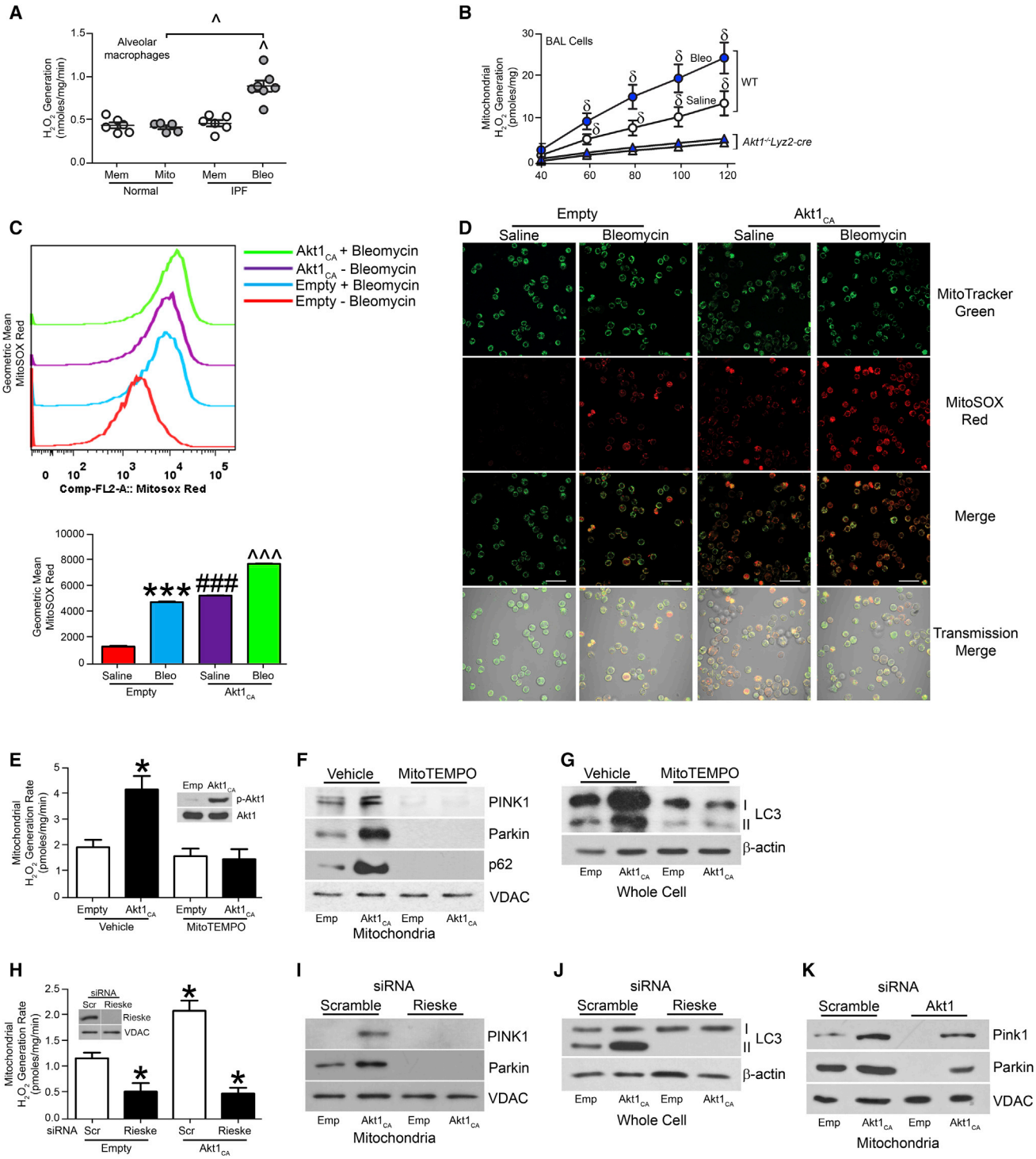

Figure 5. Akt1-Meditated ROS Generation Induces Mitophagy in Macrophages

(A) H_2O_2 production was measured in membrane (mem) and mitochondrial fractions (mito) from isolated alveolar macrophages from normal subjects (n = 6 mem; n = 5 mito) and IPF patients (n = 6 mem; n = 7 mito).

(B) Mitochondria were isolated from alveolar macrophages and H_2O_2 production was measured. WT (n = 4 saline; n = 5 bleo) and *Akt1*$^{-/-}$*Lyz2-cre* mice (n = 4 saline; n = 6 bleo).

(C) Flow cytometry with MitoSOX geometric mean and (D) Representative confocal images of MH-S cells transfected with empty or $Akt1_{CA}$ vector treated with saline or bleomycin (12.5 mU/ml). Macrophages were co-stained with MitoTracker and MitoSOX. Scale bar represents 40 μm. n = 5.

(legend continued on next page)

treatment further enhanced MitoSOX intensity in cells expressing $Akt1_{CA}$ (Figure 5C). These results were confirmed visually by confocal microscopy (Figure 5D).

Verifying that ROS production induced mitophagy via Akt1, H_2O_2 production in isolated mitochondria from macrophages expressing $Akt1_{CA}$ was significantly inhibited by the mitochondrial targeted antioxidant, MitoTEMPO (Figure 5E). Immunoblot analysis showed MitoTEMPO treatment inhibited mitophagy (Figure 5F) and reduced LC3-II expression (Figure 5G) in the presence of $Akt1_{CA}$. Silencing of Rieske mRNA, encoding a mitochondrial iron-sulfur protein, significantly reduced mitochondrial H_2O_2 in the presence or absence of $Akt1_{CA}$ (Figure 5H). Immunoblot analysis revealed that silencing of Rieske mRNA abolished PINK1 and Parkin expression (Figure 5I) and decreased LC3-II expression (Figure 5J). The role of mitochondrial H_2O_2 inducing mitophagy was further confirmed using Antimycin A (Figures S5C–S5E).

Because Akt1 induces mitophagy, we assessed whether overexpression of $Akt1_{CA}$ in Akt1-deficient cells rescued mitophagy. Silencing of Akt1 mRNA resulted in absence of these markers of mitophagy, whereas $Akt1_{CA}$ overexpression partially increased PINK1 and Parkin (Figure 5K). These observations suggest Akt1-mediated mitochondrial H_2O_2 modulates macrophage mitophagy.

Mitophagy Is Required for Active TGF-β1 Expression

Because *Akt1*$^{-/-}$*Lyz2-cre* mice have reduced active TGF-β1, we determined whether this reduction was only due to Akt1 deficiency. Immunoblot analysis showed overexpression of $Akt1_{CA}$ in cells with Akt1 mRNA silencing partially rescued Akt1 expression (Figure 6A, inset). $Akt1_{CA}$ overexpression increased TGF-β1 mRNA expression (Figure 6A) and active TGF-β1 in the conditioned media (Figure 6B). Silencing of Akt1 mRNA reduced TGF-β1 below control, whereas $Akt1_{CA}$ overexpression partially rescued gene expression and activation of TGF-β1.

We determined whether the rescue of Akt1 had a physiologic effect on fibroblast differentiation. IPF fibroblasts incubated in conditioned media from macrophages overexpressing $Akt1_{CA}$ had significantly increased α-SMA, while IPF fibroblasts cultured in conditioned media from Akt1-deficient macrophages decreased α-SMA expression (Figure 6C). Conditioned media from Akt1-deficient macrophages transfected with $Akt1_{CA}$ increased α-SMA expression in IPF fibroblasts, suggesting Akt1-mediated mitophagy is linked to TGF-β1.

Because Akt1 regulates TGF-β1 mRNA expression, we investigated whether Akt1 modulated AP-1-driven transcription, as it regulates the promoter of many growth factors, including TGF-β1 (Birchenall-Roberts et al., 1990; Kim et al., 1990). We determined that Akt1 increased phosphorylation of c-Jun and nuclear localization of c-Fos (Figure S6A). This was associated with a significant increase in AP-1-driven luciferase and *Tgfb1* promoter activity (Figures S6B and S6C).

Because MitoTEMPO treatment and Parkin2 mRNA silencing inhibited mitophagy in macrophages, we assessed whether macrophage mitophagy was required for TGF-β1 mRNA expression. $Akt1_{CA}$ overexpression increased TGF-β1 mRNA expression in vehicle-treated cells, whereas inhibition of mitophagy with MitoTEMPO decreased TGF-β1 mRNA expression significantly (Figure 6D). Similarly, Parkin2 mRNA silencing significantly reduced TGF-β1 mRNA below control in the presence or absence of $Akt1_{CA}$ overexpression (Figure 6E). This was also present in vivo. Active TGF-β1 in BAL fluid from *Park2*$^{-/-}$ mice was below saline controls (Figure 6F).

Because mitophagy regulated macrophage-derived TGF-β1 mRNA expression and several growth factors can induce fibroblast differentiation and myofibroblast function, we investigated whether macrophage-derived TGF-β1 was the responsible for fibroblast differentiation. Utilizing a TGF-β1 neutralizing antibody, we reduced active TGF-β1 in BAL fluid (Figure 6G). IPF fibroblasts incubated with neutralized BAL fluid failed to differentiate, shown by markedly less α-SMA compared to the saline control (Figure 6H). The quantification of these observations showed a greater than 75 percent reduction in α-SMA expression in bleomycin-injured WT mice (Figure 6I).

This was further confirmed by assessing TGF-β1 signaling. IPF fibroblasts incubated in BAL fluid from *Akt1*$^{-/-}$*Lyz2-cre* mice lacked p-Smad2 expression compared to cells exposed to BAL fluid from bleomycin-injured WT mice (Figure 6J). In fact, p-Smad2 expression in IPF fibroblasts incubated in BAL fluid from *Akt1*$^{-/-}$*Lyz2-cre* mice was similar to cells treated with SB431542, the TGF-β type 1 receptor (ALK5) inhibitor (Figure 6K). Rapamycin-treated mice had increased active TGF-β1 in BAL fluid and bleomycin injury led to further induction (Figure S6D). In aggregate, these data indicate that Akt1-induced mitophagy in alveolar macrophages is required for macrophage-derived TGF-β1 expression, which promotes fibrosis development.

IPF Alveolar Macrophages Have Apoptosis Resistance

Macrophages in chronic disease typically exhibit apoptosis resistance, which is generally associated with disease progression (Duffield et al., 2005; Redente et al., 2014). We determined that IPF alveolar macrophages were resistant to apoptosis with greater than 85 percent less active caspase-3 compared to normal subjects (Figure 7A). Although alveolar macrophages were the primary cell type in murine BAL fluid, *Akt1*$^{-/-}$*Lyz2-cre* mice had a significant reduction in the number of alveolar macrophages compared to WT mice (Figure S7A). Moreover, macrophages isolated from bleomycin-injured WT mice had reduced caspase-3 activity compared to saline controls, whereas

(E) Mitochondrial H_2O_2, (F) PINK, Parkin, p62, and (G) LC3-I and -II expression were determined in THP-1 cells treated with vehicle or MitoTEMPO transfected with empty or $Akt1_{CA}$ vectors. Inset, Akt1 immunoblot analysis. n = 5.

(H) Mitochondrial H_2O_2, (I) mitochondrial PINK1 and Parkin, and (J) LC3-I and -II expression were measured in THP-1 cells transfected with scrambled (Scr) or Rieske siRNA in combination with empty (emp) or $Akt1_{CA}$ vectors. Inset, Rieske immunoblot analysis. n = 5.

(K) Mitochondrial PINK1 and Parkin expression were measured in THP-1 cells transfected with scrambled or Akt1 siRNA in combination with empty or $Akt1_{CA}$ vectors; n = 5. *p < 0.05 versus Vehicle+empty or Empty+scr; ***p < 0.0001 versus Empty+saline; δ, p < 0.05 *Akt1*$^{-/-}$*Lyz2-cre* +saline and *Akt1*$^{-/-}$*Lyz2-cre*+bleo; ^, p < 0.05 versus IPF+mem; ^^^, p < 0.001 versus Empty+ Bleo; ###, p < 0.0001 versus all other conditions. One-way ANOVA with Tukey's comparison. Values are mean ± SD of a minimum of three independent experiments performed in triplicate. Please see Figure S5.

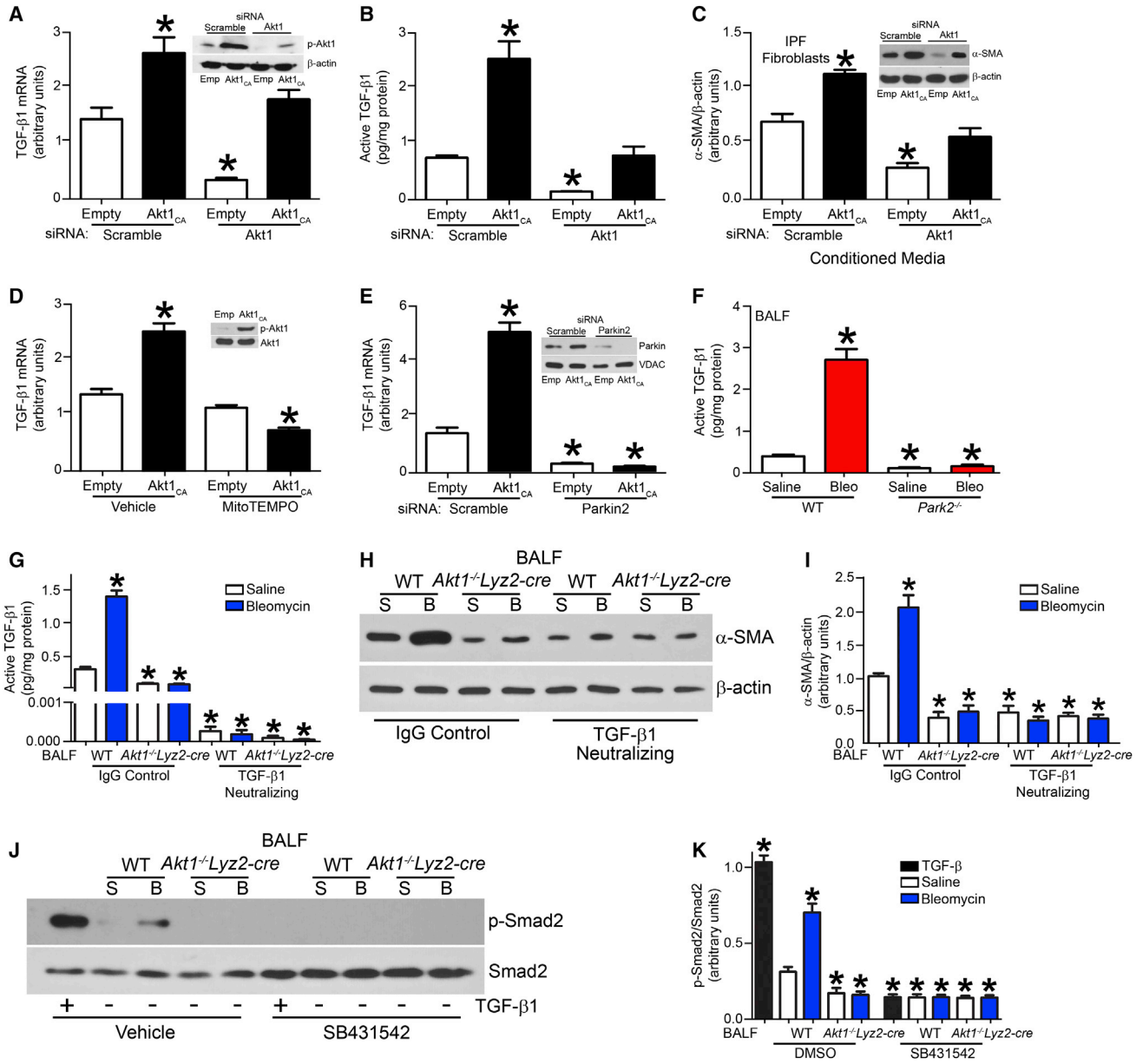

Figure 6. Macrophage Mitophagy Regulates TGF-β1 Gene Expression and Function

(A) TGF-β1 mRNA was measured in THP-1 cells transfected with scrambled or Akt1 siRNA in combination with empty or $Akt1_{CA}$ vectors; n = 5. Inset, Akt1 immunoblot analysis.

(B) Active TGF-β1 was measured by ELISA in conditioned media from THP-1 cells transfected with scrambled or Akt1 siRNA in combination with empty or $Akt1_{CA}$ vectors; n = 5.

(C) α-SMA and β-actin were measured by immunoblot (Inset) and densitometry analysis in IPF fibroblasts incubated with conditioned media from THP-1 cells transfected with scramble or Akt1 siRNA in combination with empty or $Akt1_{CA}$ vectors; n = 5.

(D) TGF-β1 mRNA expression were measured in MH-S cells expressing empty or $Akt1_{CA}$ and treated with mitoTEMPO. Inset, Akt1 overexpression verified by immunoblot analysis; n = 5.

(E) TGF-β1 mRNA expression was measured in THP-1 cells transfected with scramble or Parkin siRNA in combination with empty or $Akt1_{CA}$ vectors. Inset, Parkin2 mRNA silencing verified by immunoblot analysis; n = 5.

(F) Active TGF-β1 was measured in BAL fluid from exposed WT and *Park2*$^{-/-}$ mice; n = 5.

(G) Active TGF-β1 was measured in BAL fluid from WT and *Akt1*$^{-/-}$*Lyz2-cre* mice incubated with IgG_1 control or TGF-β1 neutralizing antibody; BAL from n = 6.

(H) Representative immunoblot and (I) densitometry analysis of IPF fibroblasts cultured in BAL fluid from saline (S) or bleomycin (B) from exposed WT and *Akt1*$^{-/-}$*Lyz2-cre* mice. BAL fluid was pre-incubated with IgG_1 control or neutralized with TGF-β1 antibody (10 μg/ml); BAL from n = 6 mice for each group on IPF fibroblasts.

(J) Representative immunoblot and (K) densitometry analysis in IPF fibroblasts pre-treated with vehicle (DMSO) or SB431542 (10 μM) and then incubated with either rhTGF- β1 (10 ng/ml) or BAL fluid from saline (S) or bleomycin (B) exposed WT and *Akt1*$^{-/-}$*Lyz2-cre* mice; BAL from n = 6 mice for each group on IPF fibroblasts. *p < 0.05 versus Scr+empty, Vehicle+empty, WT+Saline, or WT+Vehicle. One-way ANOVA with Tukey's comparison. Values are mean ± SD of a minimum of three independent experiments performed in triplicate. Please see Figure S6.

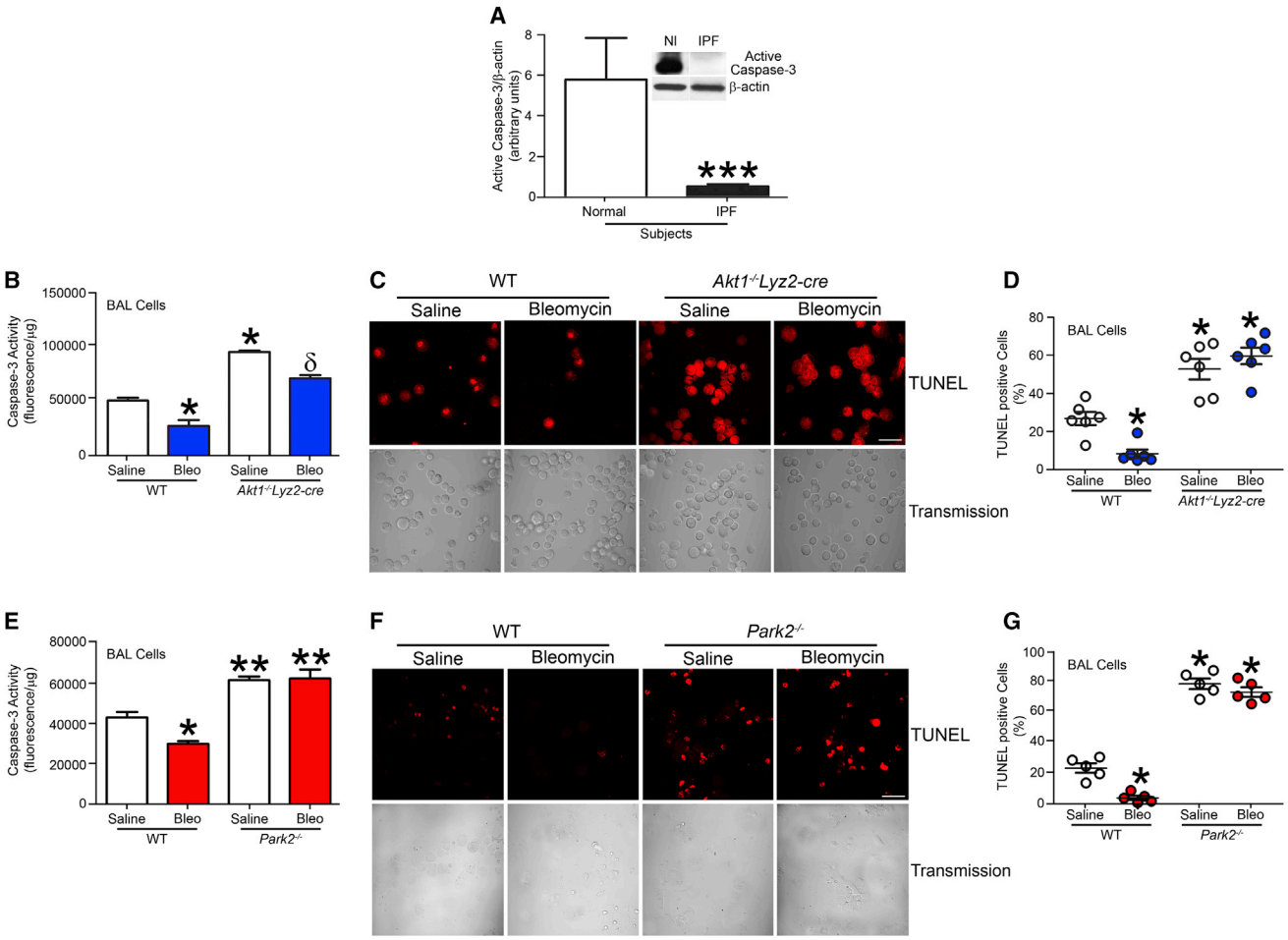

Figure 7. IPF Alveolar Macrophages Have Apoptosis Resistance

(A) Densitometry analysis in normal subjects and IPF patients (n = 5), Student's t test. Inset, representative immunoblot for cleaved caspase-3 and β-actin.

(B) Caspase-3 activity measured in alveolar macrophages isolated from exposed WT and *Akt1*$^{-/-}$*Lyz2-cre* mice; n = 4 saline, n = 6 bleo.

(C) Representative images of TUNEL staining and (D) quantification from WT and *Akt1*$^{-/-}$*Lyz2-cre* mice exposed to bleomycin or saline; n = 6, each dot represents five analyzed images. Scale bar represents 40 μm.

(F) Caspase-3 activity measured in alveolar macrophages isolated from exposed WT and *Park2*$^{-/-}$ mice. n = 5.

(G) Representative images of TUNEL staining in BAL cells and (H) quantification from exposed WT and *Park2*$^{-/-}$ mice; n = 5, each dot represents five analyzed images. Scale bar represents 40 μm. *p < 0.05 versus WT+saline; **p < 0.001 versus WT+saline and WT+bleo; ***p < 0.0001. δ, p < 0.05 versus *Akt1*$^{-/-}$*Lyz2-cre*+saline. One-way ANOVA with Tukey's comparison. Values are mean ± SD of a minimum of three independent experiments performed in triplicate. Please see Figure S7.

caspase-3 activity in macrophages from *Akt1*$^{-/-}$*Lyz2-cre* mice was significantly increased (Figure 7B). These observations were confirmed visually by TUNEL staining alveolar macrophages from WT and *Akt1*$^{-/-}$*Lyz2-cre* mice (Figure 7C). *Akt1*$^{-/-}$*Lyz2-cre* alveolar macrophages had a 6-fold increase in TUNEL-positive cells (Figure 7D). We confirmed that apoptosis was secondary to loss of Akt1. Akt1$_{CA}$ overexpression resulted in apoptosis resistance, which was further increased by bleomycin treatment (Figure S7B). These results suggest that apoptosis resistance in alveolar macrophage promotes the development of a fibrotic phenotype in mice.

To directly determine whether mitophagy is necessary for macrophage apoptosis resistance, we found that alveolar macrophages in *Park2*$^{-/-}$ mice were significantly reduced compared to WT mice (Figure S7C). Alveolar macrophages isolated from *Park2*$^{-/-}$ mice exhibited increased apoptosis, while bleomycin-injured WT mice had reduced caspase-3 activity (Figure 7F). These observations were visually confirmed by TUNEL staining (Figure 7G). *Park2*$^{-/-}$ alveolar macrophages had 17-fold greater TUNEL positive cells than WT macrophages (Figure 7H). Similar finding were found in vitro with Parkin-deficient macrophages (Figure S7D), which had 21-fold increase in TUNEL positive cells (Figure S7E).

Using an inhibitor of mitophagy, caspase-3 activity was significantly increased in macrophages treated with 3-MA compared to vehicle controls, and Akt1$_{CA}$ overexpression did not alter caspase-3 activity in the presence of 3-MA (Figure S7F). In contrast, rapamycin treatment in vivo significantly reduced caspase-3

activity in alveolar macrophages compared to vehicle-treated mice (Figure S7G). This reduction in caspase-3 activity was further enhanced by bleomycin injury. Taken together, these results suggest that mitophagy is required for apoptosis resistance in macrophages. Moreover, these observations suggest that Akt1-mediated macrophage mitophagy promotes apoptosis resistance, which regulates myofibroblast differentiation by modulating macrophage-derived TGF-β1, and thus, has a critical role in the pathogenesis of pulmonary fibrosis.

DISCUSSION

Macrophages in chronic disease typically exhibit apoptosis resistance and their prolonged survival is generally associated with disease progression. In fact, conditional macrophage depletion has been shown to attenuate models of liver and lung injury in vivo (Duffield et al., 2005; Redente et al., 2014). Phagocytosis of apoptotic cells, which are frequently present in tissue injury, also augments cell survival (Weigert et al., 2006). Our observations suggest that dysfunctional mitochondria are removed in alveolar macrophages, promoting apoptosis resistance during the fibrotic process, and Akt1-mediated mitophagy modulates TGF-β1 and the effector cells, myofibroblasts.

Mitophagy is a cell survival mechanism that is increased in conditions of stress to attempt to retain cell homeostasis. Genetic deletion of *PINK1* and *PARK2* leads to progressive mitochondrial damage that is associated with Parkinson's disease (Lin and Beal, 2006). Mitophagy is known to play an important role in many physiological processes. It has been implicated in aging, tumorigenesis, and it contributes to many diseases, including the neurological diseases Parkinson's, Alzheimer's, and Huntington's, and immunological disorders (Cui et al., 2006; Inami et al., 2011; Lemasters, 2005; Lin and Beal, 2006; Maurer et al., 2000; Zhou et al., 2011). Mitophagy is impaired in the IPF lungs, and the role mitophagy plays in alveolar macrophages in pulmonary fibrosis is not known (Araya et al., 2013; Bueno et al., 2015; Patel et al., 2015; Ricci et al., 2013). The fact that IPF patients taking the rapamycin analog, everolimus, had progression of disease (Malouf et al., 2011) uncovers the fact that mitophagy contributes to macrophage apoptosis resistance, which appears to be an important feature in the pathogenesis of the disease.

Akt activation is strongly associated with regulating survival and differentiation of myofibroblasts in the setting of pulmonary fibrosis, as it is known to regulate many fibrotic remodeling processes (Xia et al., 2008). Studies indicate TGF-β1 regulates Akt activation in myofibroblasts, and inhibition of Akt diminishes TGF-β1-induced fibrosis (Horowitz et al., 2007; Kang et al., 2007). Integrin αvβ6, expressed on epithelial cells, has been implicated in regulating the local activity of latent TGF-β1 in response to lung injury (Munger et al., 1999). $\beta 6^{-/-}$ mice are protected from bleomycin-induced pulmonary fibrosis due to the inability to activate TGF-β1. Our results do not refute the necessity of αvβ6 in activating latent TGF-β1. Rather, our data demonstrate that alveolar macrophages are the primary source of TGF-β1. However, no study to our knowledge, has implicated Akt1 in regulating TGF-β1 production in macrophages, especially in the pathogenesis of pulmonary fibrosis.

TGF-β1 is known to decrease autophagy in human lung fibroblasts by activation of Akt in the IPF lung (Araya et al., 2013; Mi et al., 2011). Studies suggest that mitophagy is induced in type II alveolar epithelial cells treated with TGF-β1, and TGF-β1 increases autophagy in other cell types as well (Ghavami et al., 2015; Patel et al., 2015). Furthermore, Akt is known to dampen TGF-β1 signaling by direct interaction with SMAD3 (Conery et al., 2004; Remy et al., 2004). This diversity in Akt, TGF-β1, and autophagy might be cell-type or stimulus specific; however, our observations show that Akt1 regulates the expression of macrophage-derived TGF-β1 by increasing mitophagy, which results in the development of a fibrotic phenotype in mice.

Pulmonary fibrosis is characterized by aberrant wound healing leading to collagen deposition and distortion of normal lung architecture. Macrophages are known to regulate multiple cell types by secreting growth factors and cytokines (Bitterman et al., 1982; Lemaire et al., 1986). Macrophages not only initiate an inflammatory response after injury, but they are also involved in resolution and repair of the injury. These divergent functions of macrophages are determined by their plasticity and ability to differentiate into distinct macrophage sub-populations. Anti-fibrotic macrophages generate pro-inflammatory cytokines and kill microorganisms and tumor cells, whereas pro-fibrotic macrophages are anti-inflammatory, promote angiogenesis and tissue remodeling, and can be associated with fibrotic conditions, including pulmonary fibrosis (He et al., 2013; Nair et al., 2009). In fact, pro-fibrotic macrophages are often found in the fibrotic tissues (He et al., 2013; Redente et al., 2014). Studies show that alternatively activated macrophages have a prolonged survival because they are involved in repair of injured tissue (Duffield et al., 2005; Redente et al., 2014). In aggregate, the observations in this study suggest that Akt1-mediated macrophage mitophagy is linked to apoptosis resistance, pro-fibrotic polarization, and is required for fibrosis development.

EXPERIMENTAL PROCEDURES

Human Subjects

We obtained human alveolar macrophages, as previously described (He et al., 2011), from normal subjects and IPF patients under an approved protocol by the Human Subjects Institutional Review Board of the University of Iowa Carver College of Medicine and the University of Alabama at Birmingham. Primary alveolar macrophages and lung fibroblasts isolated as previously described (Hecker et al., 2009; Osborn-Heaford et al., 2015), from lung of human subjects with IPF.

Mice

Wild-type C57BL/6, *Akt1*$^{+/-}$ (B6.129P2-Akt1^{tm1Mbb}/J), and *Park2*$^{-/-}$ (B6.129S4-Park2^{tm1Shn}/J) mice were purchased from JAX Laboratories. *Akt1*$^{-/-}$*Lyz2-cre* and *Tgfb1*$^{-/-}$*Lyz2-cre* mice were generated by selective disruption of *Akt1* or *Tgfb1* gene in the cells of the granulocyte and/or monocyte lineage. All protocols were approved by the University of Iowa and the University of Alabama at Birmingham Institutional Animal Care and Use Committee. Mice were intratracheally administered 1.75-2 U/kg of bleomycin or saline, as a negative control, as previously described.

Cell Culture

Human monocyte (THP-1) and mouse alveolar macrophage (MH-S) cell lines were obtained from American Type Culture Collection. Cell culture maintenance is listed in Supplemental Experimental Procedures.

Quantitative Real-Time PCR

Total RNA was isolated, reverse transcribed, and quantitative real-time PCR was performed as described previously (Larson-Casey et al., 2014). Data was calculated by the cycle threshold ($^{\Delta\Delta}$CT) method, normalized to β-actin

or HPRT, and expressed in arbitrary units. Primer information is listed in Supplemental Experimental Procedures.

Plasmids, Transfections, and Luciferase Assays

The constitutively active Akt1 "Genbank: NM_005163.2" plasmid ($Akt1_{CA}$) was a generous gift from Rama K. Mallampalli (Department of Medicine, University of Pittsburgh). Human AP-1 and TGF-β1 gene expression were evaluated using a luciferase reporter plasmid as previously described (Carter et al., 2001; Jaffer et al., 2015). Cells were transfected using X-treme GENE 9 Transfection Reagent (Roche Applied Scientific) according to the manufacturer's protocol. Renilla and firefly luciferase activity was determined in cell lysates using the Dual Luciferase reporter assay kit (Promega) and normalized to control (firefly).

Small Interfering RNA (siRNA)

Cells were transfected with 100 nM scramble, human Akt1, human Parkin2, or human Rieske siRNA duplex (IDT), utilizing Dharmafect 2 or Duo (Thermo Scientific) according to manufacturer's protocol. 8 hr after transfection, media was replaced and cells were allowed to recover for 24-72 hr.

Determination of H_2O_2 Generation

H_2O_2 production was determined fluorometrically, as previously described (Larson-Casey et al., 2014). ROS was also measured in live cells using dihydroethidium derivative (MitoSOX) (Molecular Probes) at 5 μM. Mitochondrial localization of the staining was confirmed by colocalization with MitoTracker green (Molecular Probes) at 50 nM. Cells were imaged using Zeiss LSM 710 confocal microscope; all images were taken at the same time and same imaging settings. Mitochondrial H_2O_2 was determined using MitoTEMPO (Enzo) at 10 μM.

Flow Cytometry

Macrophage apoptosis was assessed using Annexin V staining (BD Biosciences), according to the manufacturer's recommendations. For determination of mitochondrial superoxide, cells were incubated with MitoSOX red (5 μM) and MitoTracker green (50 nM) for mitochondrial localization. Data (30,000 events) were acquired on Becton Dickinson LSR II flow cytometer using FACS Diva software (BD Biosciences) and were further analyzed using FlowJo 8.5 (Tree Star).

Assay for α-SMA Expression

Normal or IPF fibroblasts were incubated in equal concentrations of BAL fluid from WT and *Akt1*$^{-/-}$*Lyz2-cre* or *Tgfb1*$^{-/-}$*Lyz2-cre* mice exposed to saline or bleomycin or conditioned media from transfected macrophages. Fibroblasts were harvested after 24 hr of incubation with BAL fluid or conditioned media and lysates were analyzed for α-SMA expression.

TGF-β1 Neutralization

BAL fluid from WT and *Akt1*$^{-/-}$*Lyz2-cre* mice was incubated with TGF-β1 neutralizing antibody (clone #9016) or immunoglobulin G_1 (IgG_1) control antibody (clone #11711) (R & D Systems) and then placed on IPF fibroblasts. IPF fibroblasts were incubated with DMSO or SB 431542 (TGF-β type 1 receptor inhibitor) (R&D Systems) and then cultured with BAL fluid from WT and *Akt1*$^{-/-}$*Lyz2-cre* mice.

Transmission Electron Microscopy

Macrophages were fixed in 2.5% paraformaldehyde and 2.5% glutaraldehyde in Sorenson's phosphate buffer at pH 7.4. Cells were processed and sectioned with a diamond knife (Diatome, Electron Microscopy Sciences) at 70–80 nm and sections were placed on copper mesh grids. Sections were stained with uranyl acetate and lead citrate for contrast and viewed on a Tecnai Twin 120kv TEM (FEI).

Statistical Analysis

Statistical comparisons were performed using either an unpaired two-tailed t test or one-way ANOVA with a Tukey's post hoc test. All statistical analysis was expressed as ± SD and $p < 0.05$ was considered to be significant.

SUPPLEMENTAL INFORMATION

Supplemental Information includes seven figures and Supplemental Experimental Procedures and can be found with this article online at http://dx.doi.org/10.1016/j.immuni.2016.01.001.

AUTHOR CONTRIBUTIONS

J.L.C. and A.B.C. developed the concept and design of the study. J.L.C., J.S.D., A.J.R., V.J.T., and A.B.C. assisted with analysis and interpretation of experiments and results. J.L.C. and A.B.C. wrote the manuscript.

ACKNOWLEDGMENTS

We thank Dr. Stephen Barnes and Ray Moore II with the UAB Targeted Metabolomics & Proteomics Laboratory for assistance with GSH analysis by HPLC, Melissa Foley Chimento and the UAB High Resolution Imaging Facility for assistance with TEM, and M. Taaj Khan for assistance in generating the *Tgfb1*$^{-/-}$*Lyz2-cre* mice. Research reported in this publication was supported in whole or in part, by National Institute of Health Grants 2R01ES015981-08 to A.B.C., 2T32HL105346-06 to the division of Pulmonary, Allergy, and Critical Care, and the Targeted Metabolomics and Proteonomics Laboratory supported by P30DK079337 (UAB O'Brien Acute Kidney Center), the UAB Lung Health Center, and the UAB Center for Free Radical Biology. This work was also supported by a Merit Review from the Department of Veterans Affairs, Veterans Health Administration, Office of Research and Development, and Biological Laboratory Research and Development BX001135-03 to A.B.C.

Received: August 20, 2015
Revised: November 17, 2015
Accepted: January 4, 2016
Published: February 23, 2016

REFERENCES

Araya, J., Kojima, J., Takasaka, N., Ito, S., Fujii, S., Hara, H., Yanagisawa, H., Kobayashi, K., Tsurushige, C., Kawaishi, M., et al. (2013). Insufficient autophagy in idiopathic pulmonary fibrosis. Am. J. Physiol. Lung Cell. Mol. Physiol. *304*, L56–L69.

Birchenall-Roberts, M.C., Ruscetti, F.W., Kasper, J., Lee, H.D., Friedman, R., Geiser, A., Sporn, M.B., Roberts, A.B., and Kim, S.J. (1990). Transcriptional regulation of the transforming growth factor beta 1 promoter by v-src gene products is mediated through the AP-1 complex. Mol. Cell. Biol. *10*, 4978–4983.

Bitterman, P.B., Rennard, S.I., Hunninghake, G.W., and Crystal, R.G. (1982). Human alveolar macrophage growth factor for fibroblasts. Regulation and partial characterization. J. Clin. Invest. *70*, 806–822.

Bueno, M., Lai, Y.C., Romero, Y., Brands, J., St Croix, C.M., Kamga, C., Corey, C., Herazo-Maya, J.D., Sembrat, J., Lee, J.S., et al. (2015). PINK1 deficiency impairs mitochondrial homeostasis and promotes lung fibrosis. J. Clin. Invest. *125*, 521–538.

Carter, A.B., Tephly, L.A., and Hunninghake, G.W. (2001). The absence of activator protein 1-dependent gene expression in THP-1 macrophages stimulated with phorbol esters is due to lack of p38 mitogen-activated protein kinase activation. J. Biol. Chem. *276*, 33826–33832.

Chang, A.L., Ulrich, A., Suliman, H.B., and Piantadosi, C.A. (2015). Redox regulation of mitophagy in the lung during murine Staphylococcus aureus sepsis. Free Radic. Biol. Med. *78*, 179–189.

Chen, Y., Azad, M.B., and Gibson, S.B. (2009). Superoxide is the major reactive oxygen species regulating autophagy. Cell Death Differ. *16*, 1040–1052.

Chen, B.B., Coon, T.A., Glasser, J.R., Zou, C., Ellis, B., Das, T., McKelvey, A.C., Rajbhandari, S., Lear, T., Kamga, C., et al. (2014). E3 ligase subunit Fbxo15 and PINK1 kinase regulate cardiolipin synthase 1 stability and mitochondrial function in pneumonia. Cell Rep. *7*, 476–487.

Collard, H.R., Ward, A.J., Lanes, S., Cortney Hayflinger, D., Rosenberg, D.M., and Hunsche, E. (2012). Burden of illness in idiopathic pulmonary fibrosis. J. Med. Econ. *15*, 829–835.

Collard, H.R., Chen, S.Y., Yeh, W.S., Li, Q., Lee, Y.C., Wang, A., and Raghu, G. (2015). Health care utilization and costs of idiopathic pulmonary fibrosis in U.S. Medicare beneficiaries aged 65 years and older. Ann. Am. Thorac. Soc. *12*, 981–987.

Conery, A.R., Cao, Y., Thompson, E.A., Townsend, C.M., Jr., Ko, T.C., and Luo, K. (2004). Akt interacts directly with Smad3 to regulate the sensitivity to TGF-beta induced apoptosis. Nat. Cell Biol. *6*, 366–372.

Cui, L., Jeong, H., Borovecki, F., Parkhurst, C.N., Tanese, N., and Krainc, D. (2006). Transcriptional repression of PGC-1alpha by mutant huntingtin leads to mitochondrial dysfunction and neurodegeneration. Cell *127*, 59–69.

Duffield, J.S., Forbes, S.J., Constandinou, C.M., Clay, S., Partolina, M., Vuthoori, S., Wu, S., Lang, R., and Iredale, J.P. (2005). Selective depletion of macrophages reveals distinct, opposing roles during liver injury and repair. J. Clin. Invest. *115*, 56–65.

Ghavami, S., Cunnington, R.H., Gupta, S., Yeganeh, B., Filomeno, K.L., Freed, D.H., Chen, S., Klonisch, T., Halayko, A.J., Ambrose, E., et al. (2015). Autophagy is a regulator of TGF-beta1-induced fibrogenesis in primary human atrial myofibroblasts. Cell death & disease *6*, e1696.

Govindarajan, B., Sligh, J.E., Vincent, B.J., Li, M., Canter, J.A., Nickoloff, B.J., Rodenburg, R.J., Smeitink, J.A., Oberley, L., Zhang, Y., et al. (2007). Overexpression of Akt converts radial growth melanoma to vertical growth melanoma. J. Clin. Invest. *117*, 719–729.

He, C., Murthy, S., McCormick, M.L., Spitz, D.R., Ryan, A.J., and Carter, A.B. (2011). Mitochondrial Cu,Zn-superoxide dismutase mediates pulmonary fibrosis by augmenting H2O2 generation. J. Biol. Chem. *286*, 15597–15607.

He, C., Ryan, A.J., Murthy, S., and Carter, A.B. (2013). Accelerated development of pulmonary fibrosis via Cu,Zn-superoxide dismutase-induced alternative activation of macrophages. J. Biol. Chem. *288*, 20745–20757.

Hecker, L., Vittal, R., Jones, T., Jagirdar, R., Luckhardt, T.R., Horowitz, J.C., Pennathur, S., Martinez, F.J., and Thannickal, V.J. (2009). NADPH oxidase-4 mediates myofibroblast activation and fibrogenic responses to lung injury. Nat. Med. *15*, 1077–1081.

Horowitz, J.C., Rogers, D.S., Sharma, V., Vittal, R., White, E.S., Cui, Z., and Thannickal, V.J. (2007). Combinatorial activation of FAK and AKT by transforming growth factor-beta1 confers an anoikis-resistant phenotype to myofibroblasts. Cell. Signal. *19*, 761–771.

Inami, Y., Waguri, S., Sakamoto, A., Kouno, T., Nakada, K., Hino, O., Watanabe, S., Ando, J., Iwadate, M., Yamamoto, M., et al. (2011). Persistent activation of Nrf2 through p62 in hepatocellular carcinoma cells. J. Cell Biol. *193*, 275–284.

Jaffer, O.A., Carter, A.B., Sanders, P.N., Dibbern, M.E., Winters, C.J., Murthy, S., Ryan, A.J., Rokita, A.G., Prasad, A.M., Zabner, J., et al. (2015). Mitochondrial-targeted antioxidant therapy decreases transforming growth factor-β-mediated collagen production in a murine asthma model. Am. J. Respir. Cell Mol. Biol. *52*, 106–115.

Jain, M., Rivera, S., Monclus, E.A., Synenki, L., Zirk, A., Eisenbart, J., Feghali-Bostwick, C., Mutlu, G.M., Budinger, G.R., and Chandel, N.S. (2013). Mitochondrial reactive oxygen species regulate transforming growth factor-β signaling. J. Biol. Chem. *288*, 770–777.

Kang, H.R., Lee, C.G., Homer, R.J., and Elias, J.A. (2007). Semaphorin 7A plays a critical role in TGF-beta1-induced pulmonary fibrosis. J. Exp. Med. *204*, 1083–1093.

Kim, S.J., Angel, P., Lafyatis, R., Hattori, K., Kim, K.Y., Sporn, M.B., Karin, M., and Roberts, A.B. (1990). Autoinduction of transforming growth factor beta 1 is mediated by the AP-1 complex. Mol. Cell. Biol. *10*, 1492–1497.

Kim, S.I., Na, H.J., Ding, Y., Wang, Z., Lee, S.J., and Choi, M.E. (2012). Autophagy promotes intracellular degradation of type I collagen induced by transforming growth factor (TGF)-β1. J. Biol. Chem. *287*, 11677–11688.

Larson-Casey, J.L., Murthy, S., Ryan, A.J., and Carter, A.B. (2014). Modulation of the mevalonate pathway by akt regulates macrophage survival and development of pulmonary fibrosis. J. Biol. Chem. *289*, 36204–36219.

Lee, S.J., Ryter, S.W., Xu, J.F., Nakahira, K., Kim, H.P., Choi, A.M., and Kim, Y.S. (2011). Carbon monoxide activates autophagy via mitochondrial reactive oxygen species formation. Am. J. Respir. Cell Mol. Biol. *45*, 867–873.

Lemaire, I., Beaudoin, H., Massé, S., and Grondin, C. (1986). Alveolar macrophage stimulation of lung fibroblast growth in asbestos-induced pulmonary fibrosis. Am. J. Pathol. *122*, 205–211.

Lemasters, J.J. (2005). Selective mitochondrial autophagy, or mitophagy, as a targeted defense against oxidative stress, mitochondrial dysfunction, and aging. Rejuvenation Res. *8*, 3–5.

Lin, M.T., and Beal, M.F. (2006). Mitochondrial dysfunction and oxidative stress in neurodegenerative diseases. Nature *443*, 787–795.

Malouf, M.A., Hopkins, P., Snell, G., and Glanville, A.R.; Everolimus in IPF Study Investigators (2011). An investigator-driven study of everolimus in surgical lung biopsy confirmed idiopathic pulmonary fibrosis. Respirology *16*, 776–783.

Maurer, I., Zierz, S., and Möller, H.J. (2000). A selective defect of cytochrome c oxidase is present in brain of Alzheimer disease patients. Neurobiol. Aging *21*, 455–462.

Mi, S., Li, Z., Yang, H.Z., Liu, H., Wang, J.P., Ma, Y.G., Wang, X.X., Liu, H.Z., Sun, W., and Hu, Z.W. (2011). Blocking IL-17A promotes the resolution of pulmonary inflammation and fibrosis via TGF-beta1-dependent and -independent mechanisms. J. Immunol. *187*, 3003–3014.

Mizumura, K., Cloonan, S.M., Nakahira, K., Bhashyam, A.R., Cervo, M., Kitada, T., Glass, K., Owen, C.A., Mahmood, A., Washko, G.R., et al. (2014). Mitophagy-dependent necroptosis contributes to the pathogenesis of COPD. J. Clin. Invest. *124*, 3987–4003.

Munger, J.S., Huang, X., Kawakatsu, H., Griffiths, M.J., Dalton, S.L., Wu, J., Pittet, J.F., Kaminski, N., Garat, C., Matthay, M.A., et al. (1999). The integrin alpha v beta 6 binds and activates latent TGF beta 1: a mechanism for regulating pulmonary inflammation and fibrosis. Cell *96*, 319–328.

Nair, M.G., Du, Y., Perrigoue, J.G., Zaph, C., Taylor, J.J., Goldschmidt, M., Swain, G.P., Yancopoulos, G.D., Valenzuela, D.M., Murphy, A., et al. (2009). Alternatively activated macrophage-derived RELM-alpha is a negative regulator of type 2 inflammation in the lung. J. Exp. Med. *206*, 937–952.

Narendra, D., Tanaka, A., Suen, D.F., and Youle, R.J. (2008). Parkin is recruited selectively to impaired mitochondria and promotes their autophagy. J. Cell Biol. *183*, 795–803.

Osborn-Heaford, H.L., Ryan, A.J., Murthy, S., Racila, A.M., He, C., Sieren, J.C., Spitz, D.R., and Carter, A.B. (2012). Mitochondrial Rac1 GTPase import and electron transfer from cytochrome c are required for pulmonary fibrosis. J. Biol. Chem. *287*, 3301–3312.

Osborn-Heaford, H.L., Murthy, S., Gu, L., Larson-Casey, J.L., Ryan, A.J., Shi, L., Glogauer, M., Neighbors, J.D., Hohl, R., and Brent Carter, A. (2015). Targeting the isoprenoid pathway to abrogate progression of pulmonary fibrosis. Free Radic. Biol. Med. *86*, 47–56.

Patel, A.S., Song, J.W., Chu, S.G., Mizumura, K., Osorio, J.C., Shi, Y., El-Chemaly, S., Lee, C.G., Rosas, I.O., Elias, J.A., et al. (2015). Epithelial cell mitochondrial dysfunction and PINK1 are induced by transforming growth factor-beta1 in pulmonary fibrosis. PLoS ONE *10*, e0121246.

Raghu, G., Nyberg, F., and Morgan, G. (2004). The epidemiology of interstitial lung disease and its association with lung cancer. Br. J. Cancer *91* (*Suppl 2*), S3–S10.

Redente, E.F., Keith, R.C., Janssen, W., Henson, P.M., Ortiz, L.A., Downey, G.P., Bratton, D.L., and Riches, D.W. (2014). Tumor necrosis factor-α accelerates the resolution of established pulmonary fibrosis in mice by targeting profibrotic lung macrophages. Am. J. Respir. Cell Mol. Biol. *50*, 825–837.

Remy, I., Montmarquette, A., and Michnick, S.W. (2004). PKB/Akt modulates TGF-beta signalling through a direct interaction with Smad3. Nat. Cell Biol. *6*, 358–365.

Ricci, A., Cherubini, E., Scozzi, D., Pietrangeli, V., Tabbì, L., Raffa, S., Leone, L., Visco, V., Torrisi, M.R., Bruno, P., et al. (2013). Decreased expression of autophagic beclin 1 protein in idiopathic pulmonary fibrosis fibroblasts. J. Cell. Physiol. *228*, 1516–1524.

Schwartz, D.A., Davis, C.S., Merchant, J.A., Bunn, W.B., Galvin, J.R., Van Fossen, D.S., Dayton, C.S., and Hunninghake, G.W. (1994). Longitudinal changes in lung function among asbestos-exposed workers. Am. J. Respir. Crit. Care Med. *150*, 1243–1249.

Vives-Bauza, C., Zhou, C., Huang, Y., Cui, M., de Vries, R.L., Kim, J., May, J., Tocilescu, M.A., Liu, W., Ko, H.S., et al. (2010). PINK1-dependent recruitment of Parkin to mitochondria in mitophagy. Proc. Natl. Acad. Sci. USA *107*, 378–383.

Wang, Y., Nartiss, Y., Steipe, B., McQuibban, G.A., and Kim, P.K. (2012). ROS-induced mitochondrial depolarization initiates PARK2/PARKIN-dependent mitochondrial degradation by autophagy. Autophagy *8*, 1462–1476.

Wauer, T., Simicek, M., Schubert, A., and Komander, D. (2015). Mechanism of phospho-ubiquitin-induced PARKIN activation. Nature *524*, 370–374.

Weigert, A., Johann, A.M., von Knethen, A., Schmidt, H., Geisslinger, G., and Brüne, B. (2006). Apoptotic cells promote macrophage survival by releasing the antiapoptotic mediator sphingosine-1-phosphate. Blood *108*, 1635–1642.

West, A.P., Brodsky, I.E., Rahner, C., Woo, D.K., Erdjument-Bromage, H., Tempst, P., Walsh, M.C., Choi, Y., Shadel, G.S., and Ghosh, S. (2011). TLR signalling augments macrophage bactericidal activity through mitochondrial ROS. Nature *472*, 476–480.

Xia, H., Diebold, D., Nho, R., Perlman, D., Kleidon, J., Kahm, J., Avdulov, S., Peterson, M., Nerva, J., Bitterman, P., and Henke, C. (2008). Pathological integrin signaling enhances proliferation of primary lung fibroblasts from patients with idiopathic pulmonary fibrosis. J. Exp. Med. *205*, 1659–1672.

Zhou, R., Yazdi, A.S., Menu, P., and Tschopp, J. (2011). A role for mitochondria in NLRP3 inflammasome activation. Nature *469*, 221–225.